Lattice site location and annealing behavior of implanted Ca and Sr in GaN

B. De Vries[a] and A. Vantomme
Instituut voor Kern- en Stralingsfysica, K.U. Leuven, Celestijnenlaan 200D, 3001 Leuven, Belgium and INPAC, K.U. Leuven, Celestijnenlaan 200D, 3001 Leuven, Belgium

U. Wahl
Instituto Tecnológico e Nuclear, Estrada Nacional 10, 2686-953, Sacavém, Portugal and Centro de Física Nuclear da Universidade de Lisboa, Avenida Professor Gama Pinto 2, 1649-003 Lisboa, Portugal

J. G. Correia
ITN, Estrada Nacional 10, 2686-953, Sacavém, Portugal; Centro de Física Nuclear da Universidade de Lisboa, Avenida Professor Gama Pinto 2, 1649-003 Lisboa, Portugal; and CERN-EP, 1211 Geneva 23, Switzerland

J. P. Araújo
Departamento de Física, Universidade de Porto, Rua do Campo Alegre 687, 4169-007 Porto, Portugal

W. Lojkowski and D. Kolesnikov
Institute of High Pressure Physics, Polish Academy of Sciences, Sokolowska 29/37, 01-142 Warsaw, Poland

ISOLDE Collaboration
CERN-EP, 1211 Geneva 23, Switzerland

(Received 17 February 2006; accepted 15 May 2006; published online 28 July 2006)

We report on the lattice location of ion-implanted Ca and Sr in thin films of single-crystalline wurtzite GaN. Using the emission channeling technique the angular distributions of β^- particles emitted by the radioactive isotopes ^{45}Ca ($t_{1/2}$=163.8 d) and ^{89}Sr ($t_{1/2}$=50.53 d) were monitored with a position-sensitive detector following 60 keV room-temperature implantation. Our experiments give direct evidence that ~90% of Ca and >60% of Sr atoms were occupying substitutional Ga sites with root mean square displacements of the order of 0.15–0.30 Å, i.e., larger than the expected thermal vibration amplitude of 0.074 Å. Annealing the Ca implanted samples at 1100–1350 °C in high-pressure N_2 atmosphere resulted in a better incorporation into the substitutional Ga site. The Sr implanted sample showed a small decrease in rms displacements for vacuum annealing up to 900 °C, while the substitutional fraction remained nearly constant. The annealing behavior of the rms displacements can explain why annealing temperatures above 1100 °C are needed to achieve electrical and optical activations, despite the fact that the majority of the acceptors are already located on Ga sites immediately after ion implantation. © *2006 American Institute of Physics*. [DOI: 10.1063/1.2215091]

I. INTRODUCTION

Ion implantation doping of the III-V semiconductor GaN is gaining increasing interest due to its potential for precisely controlling the distribution and concentration of dopants.[1,2] An additional advantage of ion implantation for *p*-type doping of GaN is that it does not suffer from the H passivation of acceptors, which usually accompanies incorporation during metal organic chemical vapor deposition (MOCVD).[3–5] However, the drawback of implantation is that, in order to achieve good electrical activation, the dopants must occupy regular lattice sites, and the radiation damage resulting from the implantation process has to be removed to a large extent. From a processing point of view, the situation is therefore not entirely different from doping during growth, since the activation of H-passivated acceptors also demands for post-growth annealing procedures, though at lower temperatures.

Aside from Mg, which is the preferential acceptor used in the production of light-emitting GaN devices and which is usually incorporated during growth,[5] Ca is an alternative *p*-type dopant.[6,5] The production of GaN junction field effect transistors using ion implanted Ca has already been demonstrated.[7] Good electrical activation of Ca, suggesting a high fraction of Ca on substitutional Ga sites S_{Ga}, was achieved by rapid thermal annealing of implanted samples at 1100 °C for 10–15 s. Lattice location studies on Ca implanted in GaN to fluences of 10^{15}–10^{16} cm^{-2} have already been performed with particle induced x-ray emission (PIXE) and—only on very thin GaN layers—with Rutherford backscattering channeling (RBS-C). In two studies,[8,9] only the *c*-axis channeling effects were investigated, leading to the conclusion that about 35% of Ca ions are located along the [0001] atomic rows. It was found that the Ca atoms are not perfectly aligned along the *c*-axis rows but display slight displacements perpendicular to the [0001] direction. A more detailed study by Alves *et al.*,[10] in which also the $[\bar{1}101]$ channeling patterns were examined, shows that after annealing at 1050 °C 35% of Ca atoms are located on sites that are displaced by 0.5 Å from the regular Ga sites. Finally, the results of Kobayashi and Gibson[11] indicate that more than

[a]Electronic mail: bart.devries@fys.kuleuven.be

80% of Ca ions are located near Ga sites. While they are displaced by ~0.2 Å from the Ga sites in the as-implanted state, the Ca atoms move to perfect Ga sites after annealing at 1100 °C.

Sr is—as group II impurity in GaN—also a possible acceptor. So far no work has been reported on the electrical characterization of Sr doped GaN. Pankove and Hutchby[12] did study the photoluminescence of ion-implanted GaN but did not find specific luminescence lines related to Sr. On the other hand, the lattice location of Sr implanted into GaN was determined by emission channeling. This technique makes use of the fact that charged particles emitted by radioactive isotopes in single crystals experience channeling or blocking effects along low-index crystal directions. This leads to an anisotropic particle emission yield from the crystal surface that depends in a characteristic way on the lattice sites occupied by the emitter atoms. This technique has the advantage that much smaller fluences of probe atoms need to be implanted in comparison to conventional ion beam methods. Excessive damage formation and clustering of probe atoms is thereby avoided, making emission channeling a suited technique to study the lattice sites of isolated impurities. Ronning *et al.*[13] have measured the β^- emission channeling effects from ^{89}Sr in GaN after 800 °C annealing by performing one-dimensional angular scans across three crystal axes. Only the *c*-axis measurement was analyzed, which yielded a fraction of 63% of Sr atoms located along the [0001] atomic rows.

In this work, we present a detailed lattice location study of low-fluence implanted Ca and Sr in GaN using the emission channeling technique. In contrast to the Sr study mentioned above, a position-sensitive detector was used to measure the emission channeling effects along four different crystal axes. The quantitative analysis of these results allows us to deduce the incorporation sites (and small displacements from high-symmetry lattice sites) with a significantly larger precision compared to the previous studies of both Ca and Sr implanted GaN.

II. EXPERIMENT

All investigated samples were 1–2 μm thick films of single-crystalline wurtzite GaN epitaxially grown on sapphire substrates by MOCVD. In order to investigate the lattice site location of Ca in GaN, we used the probe isotope ^{45}Ca, which was introduced by ion implantation with a radioactive beam produced at the ISOLDE facility[14] at CERN. At this institute, radioactive nuclei are produced by means of nuclear fission induced by a 1.4 GeV proton beam impinging on a UC_2 target. Following ionization in a W surface ion source and mass separation, ISOLDE provides radioactive beams of mass 45 at an energy of 60 keV, containing mainly ^{45}K and a small fraction of ^{45}Ca. We implanted four samples (A, B, C, and D) with mass 45 at room temperature to fluences of, respectively, 8.0×10^{12}, 8.4×10^{12}, 3.1×10^{12}, and 1.5×10^{13} cm^{-2}. All implantations were performed with a beam spot of 1 mm diameter, except for sample C which was implanted with a 1.6 mm spot. After implantation, ^{45}K ($t_{1/2}$ = 17.8 min, β^- end point energies of 1.2–4.2 MeV) decays to ^{45}Ca, during which the ^{45}Ca nucleus receives β^- or γ recoil energies of ~50 eV. Experimental[15] and theoretical[16] studies have shown a threshold energy of around 19 eV for a Ga displacement in GaN, with an average displacement energy of 45 eV. That means that probably a part of the ^{45}Ca atoms will not be able to escape the lattice sites previously occupied by the ^{45}K mother nuclei. After implantation, these samples were stored for a period of days to weeks before starting the experiments, which means that practically all of the ^{45}K nuclei had decayed to ^{45}Ca. The radioactive isotope ^{45}Ca subsequently decays with a half-life of 163.8 d into ^{45}Sc by the emission of β^- particles with an end point energy of 258 keV. These β^- particles were recorded by the position-sensitive Si detection system described in Ref. 17.

In order to determine the lattice site of Sr, a GaN film (sample E) was doped with the radioactive probe ^{89}Sr. Similar to the situation with ^{45}Ca, sample E was implanted with a mass separated ion beam containing a mixture of ^{89}Rb and ^{89}Sr to a fluence of 1.8×10^{13} cm^{-2} using the same setup and parameters as mentioned above. The recoil energy received by the ^{89}Sr nucleus during the decay of the short-lived isotope ^{89}Rb ($t_{1/2}$=15.15 min) ranges from 0 to 120 eV, which implies that a fraction of the ^{89}Sr atoms will probably still inherit the ^{89}Rb sites. After implantation, the sample was stored for 19 d before starting the measurements, which means that practically all of the ^{89}Rb had decayed to ^{89}Sr. During the subsequent decay of ^{89}Sr ($t_{1/2}$=50.53 d), β^- particles are emitted with an end point energy of 1495 keV. By measuring the angular emission yields of these electrons, the lattice site of Sr in GaN could be determined.

The channeling patterns presented in this work were recorded along four crystal axes that are suitable for emission channeling in GaN: [0001], [$\bar{1}$102], [$\bar{1}$101], and [$\bar{2}$113]. In addition to recording the emission yields after room-temperature implantation, all samples were remeasured after one or more annealing steps. All annealings up to 1050 °C were performed in vacuum ($<10^{-6}$ mbar) for 10 min. Some of the samples were also subjected to higher temperature annealings under high-pressure (1.0–1.1 GPa) N_2 atmosphere up to 1350 °C. These annealings were performed at the Institute of High Pressure Physics. The measurements of the angular emission yields were always performed at room temperature.

A known difficulty of emission channeling is assessing the fraction of electrons that reach the detector after they have backscattered inside the sample, the sample holder, or by other parts of the vacuum setup. These electrons will produce a rather isotropic background to the measured channeling patterns. Without proper knowledge of this contribution, it is impossible to obtain quantitative results of lattice site occupancy. In the case of monoenergetic particles, it is possible, to a large extent, to distinguish channeled and scattered particles: Since most scattered electrons will lose a significant amount of energy, one can discriminate them by applying energy windows to the experimental data. However, because of the continuous nature of β^- energy spectra, another approach is necessary for these experiments. We have quantified the scattering background by means of a Monte Carlo computer code based on the GEANT4 toolkit.[18] In these

simulations, the composition and geometry of the sample, the sample holder, the detector, and the major parts of the vacuum setup were taken into account. In addition to the scattering, the natural background radiation was also accounted for ^{45}Ca, because of the low detection count rate of electrons emitted by that isotope. This correction introduces an additional isotropic background contribution. The total background correction then consists of the subtraction of a uniform background from each of the experimental channeling patterns.

In order to analyze the experimental results, theoretical angular channeling patterns were calculated by a computer code based on the "many beam" formalism.[19] This theoretical approach was initially developed for electron microscopy and was extended for use in emission channeling experiments. Emission yields were simulated for the emitter isotopes on and in between several possible lattice sites in the GaN crystal: substitutional Ga (S_{Ga}) and N (S_N) sites with different vibration amplitudes, bond-centered (BC) and antibonding (AG and AN) sites along and off the *c*-axis, and the interstitial HG, HN, T, and O sites.[20] In these simulations we used as room-temperature vibrational amplitudes of Ga and N, 0.074 and 0.081 Å, respectively. These values were derived from extended x-ray absorbtion fine structure experiments[21] and correspond to Debye temperatures of $\Theta_D(\mathrm{Ga})=343$ K and $\Theta_D(\mathrm{N})=739$ K. To approximate the continuous β^- spectrum of ^{45}Ca, we calculated theoretical yields for electron energies from 100 to 250 keV in steps of 25 keV. For the ^{89}Sr spectrum, we also used steps of 25 keV for e^- energies from 50 to 800 keV and 50 keV steps for the higher energies of up to 1400 keV. The resulting patterns were averaged taking into account the β^- energy distributions from the ^{45}Ca and ^{89}Sr decays.[22] These theoretical emission patterns were then compared to the experimental ones by means of a two-dimensional fitting procedure described elsewhere.[17]

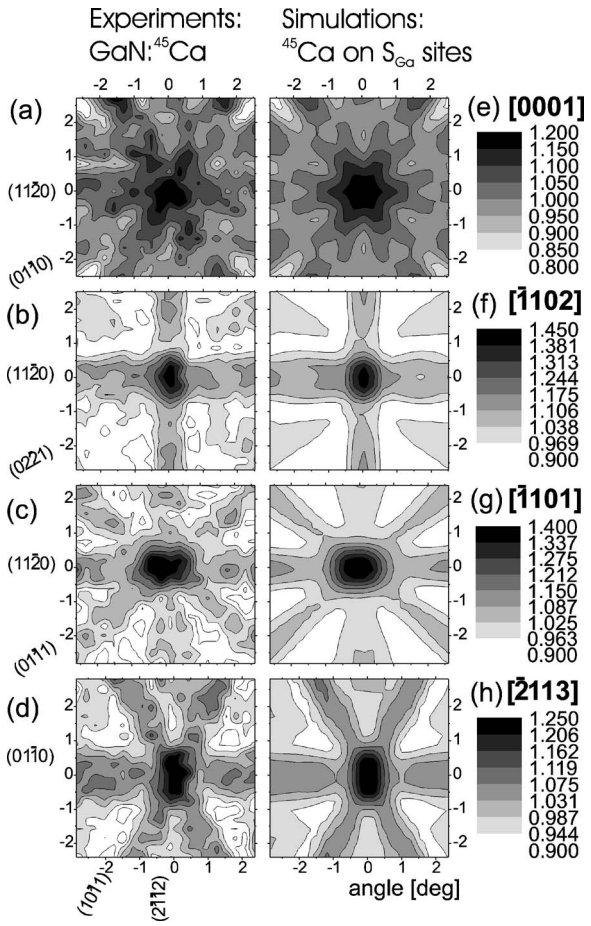

FIG. 1. [(a)–(d)] Experimental two-dimensional angular β^- yields from the ^{45}Ca implanted sample A along the [0001], [$\bar{1}$102], [$\bar{1}$101], and [$\bar{2}$113] axes. These patterns were measured after vacuum annealing at 200 °C, except the [$\bar{1}$101] pattern, which was recorded in the as-implanted state. [(e)–(h)] Best fits of theoretical patterns to the experimental yields, corresponding to 111%, 88%, 88%, and 71% of ^{45}Ca on substitutional Ga sites, with root mean square (rms) displacements of 0.18, 0.12, 0.09, and 0.16 Å, respectively.

III. RESULTS AND DISCUSSION

A. Calcium

Figure 1(a) shows the experimental angle-dependent β^- emission yield along the [0001] axis of sample A after 10 min vacuum annealing at 200 °C. The axial and planar channeling effects already give an indication that the majority of Ca atoms are situated along the *c*-axis atomic rows. Indeed, the best fit to this measurement is obtained for a theoretical emission pattern with 111% of Ca located along the *c*-axis rows with a root mean square (rms) displacement of 0.18 Å perpendicular to the *c* axis [Fig. 1(e)]. Within the experimental error bars of about 10%–20%, this shows that almost all Ca atoms are located along the *c*-axis atomic rows which are mixed rows of Ga and N. It is therefore impossible to tell if Ca is situated on substitutional Ga or N sites, or both, or even on one of the several interstitial sites along this axis. In order to obtain the full lattice site information, additional measurements were needed. Figures 1(b)–1(d) show the channeling spectra of β^- particles along the [$\bar{1}$102], [$\bar{1}$101], and [$\bar{2}$113] axes. These crystal directions consist of separate Ga and N atom rows. Because of the large difference in nuclear charge between Ga and N, the sublattice preference of Ca will have a pronounced influence on the channeling patterns along these two directions. The results of the fitting procedure show that 88%, 88%, and 71% of Ca atoms are on S_{Ga} sites with rms displacements of 0.12, 0.09, and 0.16 Å. The remainder is assumed to be located on random or low-symmetry sites. Both give a nearly isotropic contribution to the emission yield. The best fits are shown in Figs. 1(e)–1(h). Figures 2(a)–2(d) show that the theoretical yields for ^{45}Ca on S_N sites along the [$\bar{1}$102] and [$\bar{2}$113] axes are vastly different from the ones for Ca on S_{Ga} sites [Figs. 1(e)–1(h)]. The simulation for 100% of Ca on interstitial O sites produces another set of distinct channeling effects, shown in Figs. 2(e)–2(h). This clearly demonstrates the sensitivity of electron emission channeling along the four crystal axes to the lattice site occupied by Ca in GaN.

Sample A was subjected to isochronal 10 min vacuum annealing steps at 200, 400, 600, 800, and 900 °C. Afterwards it was further annealed in a high pressure (1.1 GPa) N_2 atmosphere at 1350 °C for 30 min. By remeasuring the emission yields after each annealing step, the lattice site of

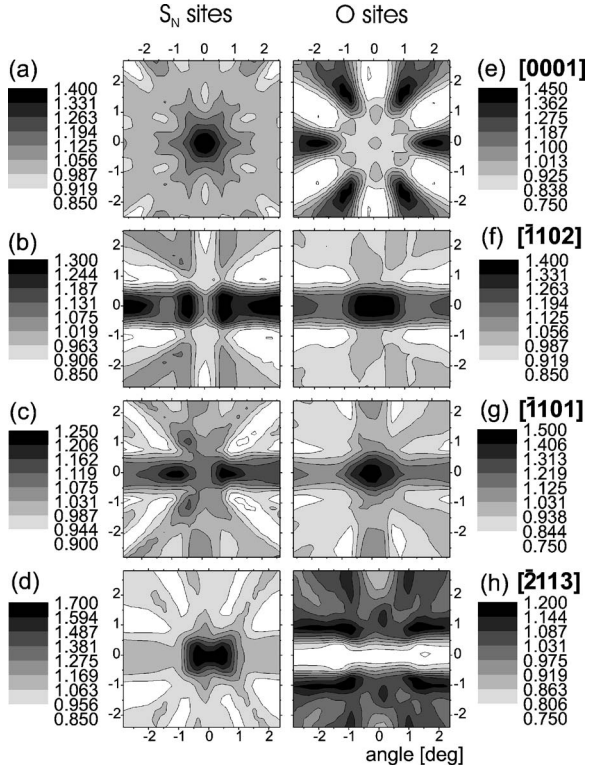

FIG. 2. Theoretically calculated angular emission yields assuming 100% of ^{45}Ca on [(a)–(d)] substitutional N sites and [(e)–(h)] O sites.

Ca could be determined as a function of annealing temperature. The other Ca implanted samples were all subjected to only one 10 min annealing step under a 1.0 GPa N_2 atmosphere: sample B at 1100 °C and samples C and D at 1150 °C. It was found that annealing the samples does not result in a change of the lattice site of Ca: The majority of Ca still resides on S_{Ga} sites, with no trace of Ca on other high-symmetry sites. Figure 3(a) shows an overview of the substitutional fractions as a function of annealing temperature. Already in the as-implanted state, our particular sample production process (including possible recoil implantation) results in large fractions (~90%) of Ca on substitutional Ga sites. Vacuum annealing and high-pressure annealing up to 1150 °C do not seem to change the S_{Ga} fraction significantly, indicating the thermal stability of Ca on Ga sites. The only exception seems to be sample D, which shows smaller S_{Ga} fractions in the as-implanted state (66%) and after 1150 °C annealing (16%). This deviation will be discussed further on. Of the other samples, only sample A displays a significant reduction in Ca substitutional fraction after going up to 1350 °C.

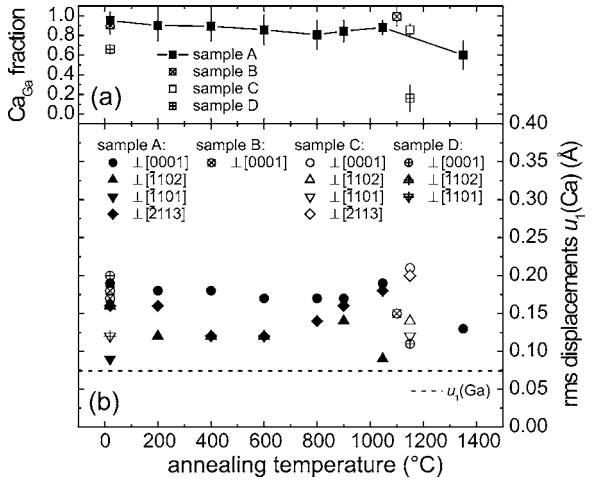

FIG. 3. (a) Fraction of ^{45}Ca on substitutional Ga sites as a function of annealing temperature. (b) Root mean square displacements from the ideal substitutional site. Note that these indicate the displacements perpendicular to the respective measurement axis. The dashed line indicates the thermal vibration amplitude of Ga in GaN: $u_1(\mathrm{Ga})=0.074$ Å.

The reverse annealing behavior displayed by sample A is most likely due to the diffusion of Ca inside the GaN layer, rather than the removal of Ca atoms from Ga sites. A redistribution of substitutional Ca atoms deeper into the layer will increase the dechanneling of electrons, since they now have a longer way to travel through the crystal, which in turn causes a decrease in the channeling effect. Since the theoretical patterns are simulated for the Gaussian implantation depth profile, the fitting procedure will lead to an apparently lower substitutional fraction if Ca diffuses into the sample. Secondary ion-mass spectroscopy (SIMS) measurements[6] have shown that there is no significant Ca redistribution for annealing temperatures up to 1125 °C (diffusion coefficient $D<2.7\times10^{-13}$ cm^2/s), which agrees with our observations that the Ca_{Ga} fraction stays almost constant up to 1150 °C. For higher annealing temperatures, no diffusion data are available for Ca. However, it is known that other implanted acceptors, Mg and Zn, begin to exhibit diffusion at ~1200 °C.[1,23,24]

An alternative explanation for the lower S_{Ga} fraction is that the surface layer was damaged during the high-pressure annealing. The defects in such a layer are also able to dechannel the electrons, leading to lower apparent Ca_{Ga} fractions. This is, however, unlikely since this sample did not show any signs of surface degradation. Sample D, on the other hand, displayed a greyish surface haze after annealing at 1150 °C, indicating that the surface layer was damaged during the annealing procedure. This can explain the anomalously low substitutional fraction after high-pressure annealing, compared to the other samples.

Apart from the substitutional fraction, the root mean square (rms) displacements from the perfect substitutional Ga site u_1(Ca) could also be deduced. The values actually correspond to displacements perpendicular to the crystal direction along which the angular yield was detected. Figure 3(b) gives an overview of the rms displacements as a function of the annealing temperature and the crystal axis. A first observation is that all measured rms displacements are larger than the room-temperature vibration amplitude of Ga in GaN, $u_1(\mathrm{Ga})=0.074$ Å. This means that the Ca atoms are displaced further from the Ga site than would be expected if only thermal vibrations were present. Theoretical calculations have shown that, for a perfect GaN crystal, Ca is stable on Ga sites with no indications of off-center relaxations.[25] Therefore, the additional displacements can be attributed to crystal defects in the vicinity of the Ca atoms. These could be native defects or, more likely, defects introduced by the ion implantation process.

There is almost no noticeable influence on the rms displacements for annealing up to 1050 °C, indicating that these temperatures are probably insufficient to completely anneal out the defects surrounding the Ca atoms. After high-pressure annealing at 1150 °C, the displacements measured for sample C were still of the same magnitude as those for lower annealing temperatures. For the other three samples only the displacement perpendicular to the *c* axis was measured after high-pressure annealing. These displacements are, however, considerably smaller. Considering that the $u_{\perp[0001]}$ values appear to be larger than those for the other axes; this suggests an actual improvement of the substitutional incorporation of the Ca atoms. This is consistent with Hall measurements that showed that electrical activation of implanted Ca (Ref. 6) and Mg (Refs. 1 and 26) can only be achieved for rapid thermal annealing temperatures $\geqslant$1100 °C. A high-pressure annealing study also showed that optical activation of implanted Mg and Zn acceptors can only be achieved for temperatures in excess of 1150–1200 °C.[24]

A last observation that was already briefly mentioned is that the apparent ordering $u_{\perp[0001]} \geqslant u_{\perp[\bar{2}113]} \geqslant u_{\perp[\bar{1}102]} \geqslant u_{\perp[\bar{1}101]}$ for annealing temperatures $\leqslant$1150 °C might indicate the presence of a small displacement anisotropy, with a preferred direction somewhere in the vicinity of the $[\bar{1}102]$ and $[\bar{1}101]$ axes.

Previously published RBS-C and PIXE studies[8–11] have shown similar but less accurate lattice location results for Ca in GaN, with Ca located on sites that are displaced from the Ga site by 0.2–0.5 Å. However, the reported substitutional Ca fractions (35%–80%) were smaller compared to our results. Most likely, this difference is due to the larger Ca fluences (10^{15}–10^{16} cm^{-2}) that are needed to carry out RBS and PIXE experiments: The increased implantation damage can give rise to a fairly large fraction of Ca atoms situated in highly damaged, disordered regions of the crystal at the expense of Ca on regular lattice sites. The decreasing displacements after annealing at 1100 °C reported by Kobayashi and Gibson[11] also agree with our observations. However, our more accurate experiments reveal that the displacements do not completely go down to the level of the vibration amplitude, implying that there are still defects present in the vicinity of the probe atoms. On the other hand, the much larger displacement of 0.5 Å after annealing at 1050 °C found by Alves *et al.*[10] is probably due to the significant increase in implantation damage caused by the significantly larger Ca fluence of 5.0×10^{15} cm^{-2}.

B. Strontium

Similar to the case described above, the angular electron emission yields from the Sr implanted sample E were detected at room temperature following isochronal annealing steps at temperatures up to 900 °C. Figures 4(a)–4(d) show the experimental patterns along four crystal axes after 800 °C annealing. Also in this case, the channeling effects along all four crystal directions indicate that Sr is situated on substitutional Ga sites. Indeed, the best fits to the experimental angular yields were obtained for 60%, 59%, 52%, and 59% of Sr on substitutional Ga sites with rms displacements of 0.16, 0.14, 0.14, and 0.18 Å [Figs. 4(e)–4(h)].

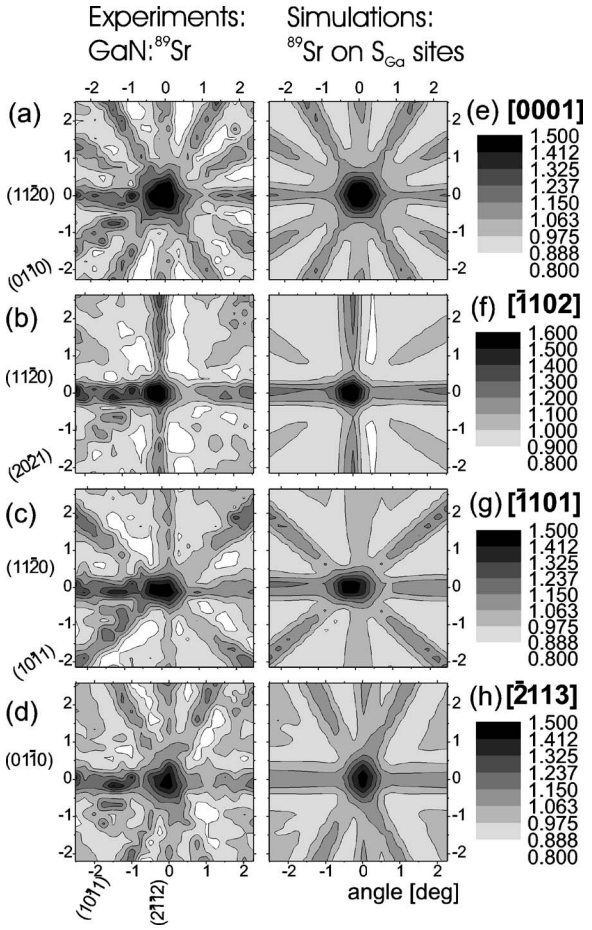

FIG. 4. [(a)–(d)] Angular β^- emission patterns from the Sr implanted sample E along the [0001], $[\bar{1}102]$, $[\bar{1}101]$, and $[\bar{2}113]$ crystal directions after 800 °C vacuum annealing. [(e)–(h)] The best fits of simulated spectra to the experimental yields corresponding to 60%, 59%, 52%, and 59% of Sr on substitutional Ga sites with rms displacements of 0.16, 0.14, 0.14, and 0.18 Å.

The sample was isochronally annealed for 10 min in vacuum at 200, 400, 600, 800, and 900 °C. After each step the emission yields along the same four crystal directions were remeasured. Figure 5(a) shows the fraction of substitutional Sr atoms as a function of annealing temperature. Al-

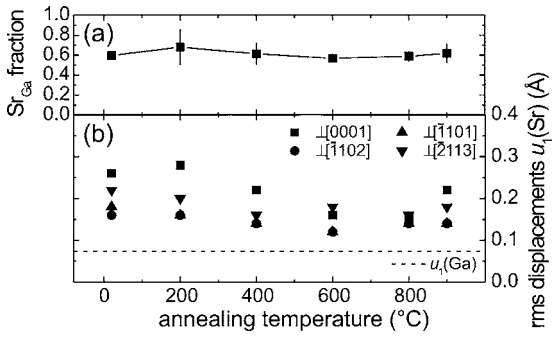

FIG. 5. (a) Fraction of ^{89}Sr on substitutional Ga sites as a function of annealing temperature. The error bars only include statistical errors. (b) Root mean square displacements from the ideal substitutional site. The dashed line indicates the thermal vibration amplitude of Ga in GaN: u_1(Ga) =0.074 Å.

ready after implantation (including transmutation doping via ^{89}Rb) around 60% of Sr atoms are located on S_{Ga} sites. Annealing up to 900 °C did not change the substitutional fraction significantly. These observations agree with the previously published emission channeling experiment on Sr implanted GaN, where 63% of Sr atoms were found along the *c*-axis atomic rows after 800 °C annealing.[13] The Sr_{Ga} fraction in Fig. 5(a) is much smaller than the 90%–100% for Ca_{Ga} mentioned above. However, the fractions that are deduced from emission channeling are prone to external influences, which was already briefly mentioned in the previous section. This is in contrast to, e.g., RBS-C, where the Ga channeling spectrum can be used as a reference to exclude external influences, such as the crystal quality. In emission channeling, the absence of such a reference can lead to large systematic errors of about 10%–20%. However, all these influences will decrease the measured fractions with respect to the physical fractions. Therefore, the values in Fig. 5 actually give a lower limit to the real substitutional fraction. Usually the systematic error is rather small (10%–20%) but may be larger for this specific isotope. Firstly, the Monte Carlo simulations that were used to estimate the scattered electron background are known to underestimate the scattering contribution for β^- emitters with high end point energies, such as the 1.5 MeV for ^{89}Sr. Another important factor is the crystalline quality of the sample: Defects can cause dechanneling, leading to lower apparent fractions. The fact that this sample was taken from the same wafer as sample D, which also showed significantly lower S_{Ga} fractions than the other Ca implanted samples, suggests that the crystalline quality is the main effect responsible for the low fractions. Therefore, it can be concluded that the majority of Sr atoms ($>60\%-70\%$) are located on S_{Ga} sites.

The root mean square displacements u_1(Sr) are displayed in Fig. 5(b). In the as-implanted state the displacements are of the order of 0.2 Å, which is somewhat larger than for ^{45}Ca. After annealing the rms displacements decrease slightly to around 0.15 Å, indicating a partial annealing of the surrounding crystal defects. However, the 900 °C annealing is not sufficient to anneal out all the damage and introduce the Sr atoms into perfect S_{Ga} sites.

IV. CONCLUSIONS

Summarizing, we have studied the lattice site location of Ca and Sr in GaN by means of electron emission channeling. Already after room-temperature implantation, the majority of Ca ($\sim$90%) was found on substitutional Ga sites with root mean square displacements of the order of 0.12–0.20 Å. The remainder was considered to occupy random sites. Annealing up to 1050 °C did not significantly change the fraction of substitutional Ca, indicating the thermal stability of Ca on Ga sites. However, high-pressure annealing at 1100–1350 °C led to a better incorporation into the Ga site. This temperature range coincides with the onset of Ca diffusion and its electrical and optical activations. A large fraction of Sr ($>60\%$) was also found on S_{Ga} sites with slightly larger rms displacements of the order of 0.15–0.30 Å. Vacuum annealing up to 900 °C did not improve the substitutional fraction but decreased the rms displacements slightly. Higher annealing temperatures are probably needed to incorporate Sr on nondisturbed Ga sites. The annealing behavior of the rms displacements explains why temperatures above 1100 °C are needed to obtain electrical and optical activations of the implanted acceptors, despite the fact that the majority is already located on Ga sites immediately after implantation.

ACKNOWLEDGMENTS

One of the authors (B.D.V.) acknowledges his fellowship from FWO-Vlaanderen and another author (U.W.) from the Foundation for Science and Technology Portugal (FCT). This work was funded by the FWO Project No. G.0210.02, the FCT Project No. CERN/FIS/43725/2001, the HPRI program (Large Scale Facility Contract No. HPRI-CT-1999-00018), the European Commission through the RENiBEl (Rare Earth doped Nitrides for high Brightness Electroluminescent emitters) network (Contract No. HPRN-CT-2001-00297), and the Centers of Excellence Programme INPAC EF/05/005.

[1] C. Ronning, E. P. Carlson, and R. F. Davis, Phys. Rep. **351**, 349 (2001).
[2] S. Kucheyev, J. S. Williams, and S. J. Pearton, Mater. Sci. Eng., R. **33**, 51 (2001).
[3] S. J. Pearton, H. Cho, F. Ren, J. I. Chyi, J. Han, and R. G. Wilson, MRS Internet J. Nitride Semicond. Res. **5S1**, W10.6 (2000).
[4] J. Chevalier, Mater. Sci. Eng., B **71**, 62 (2000).
[5] J. K. Sheu and G. C. Chi, J. Phys.: Condens. Matter **14**, R657 (2002).
[6] J. C. Zolper, R. G. Wilson, S. J. Pearton, and R. A. Stall, Appl. Phys. Lett. **68**, 1945 (1996a).
[7] J. C. Zolper, R. J. Shul, A. G. Baca, R. G. Wilson, S. J. Pearton, and R. A. Stall, Appl. Phys. Lett. **68**, 2273 (1996b).
[8] E. J. Alves, C. Liu, M. F. da Silva, J. C. Soares, R. Correia, and T. Monteiro, Mater. Res. Soc. Symp. Proc. **647**, O13.4 (2001).
[9] T. Monteiro, C. Boemare, M. J. Soares, E. Alves, and C. Liu, Physica B **308–310**, 42 (2001).
[10] E. Alves, C. Liu, E. B. Lopes, M. F. da Silva, J. C. Soares, C. Boemare, M. J. Soares, and T. Monteiro, Nucl. Instrum. Methods Phys. Res. B **190**, 625 (2002).
[11] H. Kobayashi and W. M. Gibson, Appl. Phys. Lett. **74**, 2355 (1999).
[12] J. I. Pankove and J. A. Hutchby, J. Appl. Phys. **47**, 5387 (1976).
[13] C. Ronning *et al.*, J. Appl. Phys. **87**, 2149 (2000).
[14] E. Kugler, Hyperfine Interact. **129**, 23 (2000).
[15] A. Ionascut-Nedelcescu, C. Carlone, A. Houdayer, H. J. von Bardeleben, J.-L. Cantin, and S. Raymond, IEEE Trans. Nucl. Sci. **49**, 2733 (2002).
[16] J. Nord, K. Nordlund, and J. Keinonen, Phys. Rev. B **68**, 184104 (2003).
[17] U. Wahl *et al.*, Nucl. Instrum. Methods Phys. Res. A **524**, 245 (2004).
[18] S. Agostinelli *et al.*, Nucl. Instrum. Methods Phys. Res. A **506**, 250 (2003).
[19] H. Hofsäss and G. Lindner, Phys. Rep. **201**, 121 (1991).
[20] U. Wahl, A. Vantomme, G. Langouche, J. P. Araújo, L. Peralta, J. G. Correia, and the ISOLDE Collaboration, J. Appl. Phys. **88**, 1319 (2000).
[21] A. Yoshiasa, K. Koto, H. Maeda, and T. Ishii, Jpn. J. Appl. Phys., Part 1 **36**, 781 (1997).
[22] S. Y. F. Chu, L. P. Ekström, and R. B. Firestone, Table of Radioactive Isotopes, database version, http://nucleardata.nuclear.lu.se/nucleardata/toi/, 28 February 1999.
[23] S. Strite, A. Pelzmann, T. Suski, M. Leszczynski, J. Jun, A. Rockett, M. Kamp, and K. J. Ebeling, MRS Internet J. Nitride Semicond. Res. **2**, 15 (1997).
[24] S. Porowski *et al.*, J. Phys.: Condens. Matter **14**, 11097 (2002).
[25] J. Neugebauer and C. G. Van de Walle, J. Appl. Phys. **85**, 3003 (1999).
[26] X. A. Cao *et al.*, MRS Internet J. Nitride Semicond. Res. **4S1**, G6.33 (1999).